Quantum-dot cellular automata

G. L. Snider,[a] A. O. Orlov, I. Amlani, X. Zuo, G. H. Bernstein, C. S. Lent, J. L. Merz, and W. Porod
Department of Electrical Engineering, University of Notre Dame, Notre Dame, Indiana 46556

(Received 12 October 1998; accepted 18 January 1999)

An introduction to the operation of quantum-dot cellular automata (QCA) is presented, along with recent experimental results. QCA is a transistorless computation paradigm that addresses the issues of device density and interconnection. The basic building blocks of the QCA architecture, such as AND, OR, and NOT are presented. The experimental device is a four-dot QCA cell with two electrometers. The dots are metal islands, which are coupled by capacitors and tunnel junctions. An improved design of the cell is presented in which all four dots of the cell are coupled by tunnel junctions. A noninvasive electrometer is presented which improves the sensitivity and linearity of dot potential measurements. The operation of this basic cell is confirmed by an externally controlled polarization change of the cell. © *1999 American Vacuum Society.* [S0734-2101(99)07104-3]

I. INTRODUCTION

For more than 30 years, the microelectronics industry has enjoyed dramatic improvements in the speed and size of electronic devices. This trend has long obeyed Moore's law, which predicts that the number of devices integrated on a chip will double every 18 months. Adherence to this exponential growth curve has been a monumental task requiring rapid improvements in all aspects of integrated circuit fabrication to permit manufacturers to both shrink the size of devices, and increase chip size, while maintaining acceptable yields. Since the early 1970s, the device of choice for high levels of integration has been the field effect transistor (FET). While the FET of today is a vast improvement over that of 1970, it is still used as a current switch much like the mechanical relays used by Konrad Zuse in the 1930s. At gate lengths below 0.1 μm FETs will begin to encounter fundamental effects that make further scaling difficult. A possible way for the microelectronics industry to maintain growth in device density is to change from the FET-based paradigm to one based on nanostructures. Here, instead of fighting the effects that come with feature size reduction, these effects are used to advantage. One nanostructure paradigm, proposed by Lent *et al.*,[1,2] is quantum-dot cellular automata (QCA), which employs arrays of coupled quantum dots to implement Boolean logic functions.[3,4] The advantage of QCA lies in the extremely high packing densities possible due to the small size of the dots, the simplified interconnection, and the extremely low power-delay product. Using QCA cells with dots of 20 nm diameter, an entire full adder can be placed within 1 μm^2.

A basic QCA cell consists of four quantum dots in a square array coupled by tunnel barriers. Electrons are able to tunnel between the dots, but cannot leave the cell. If two excess electrons are placed in the cell, Coulomb repulsion will force the electrons to dots on opposite corners. There are thus two energetically equivalent ground state polarizations, as shown in Fig. 1, which can be labeled logic ''0'' and ''1.'' If two cells are brought close together, Coulombic interactions between the electrons cause the cells to take on the same polarization. If the polarization of one of the cells is gradually changed from one state to the other, the second cell exhibits a highly bistable switching of its polarization, shown in Fig. 2. The simplest QCA array is a line of cells, shown in Fig. 3(a). Since the cells are capacitively coupled to their neighbors, the ground state of the line is for all cells to have the same polarization. In this state, the electrons are as widely separated as possible, giving the lowest possible energy. To use the line, an input is applied at the left end of the line, breaking the degeneracy of the ground state of the first cell and forcing it to one polarization. Since the first and second cell are now of opposite polarization, with two electrons close together, the line is in a higher energy state and all subsequent cells in the line must flip their polarization to reach the new ground state. No metastable state (where only a few cells flip) is possible in a line of cells.[2] A tremendous advantage of QCA devices is the simplified interconnect made possible by this paradigm. Since the cells communicate only with their nearest neighbors, there is no need for long interconnect lines. The inputs are applied to the cells at the edge of the system and the computation proceeds until the output appears at cells at the edge of the QCA array.

Computing in the QCA paradigm can be viewed as computing with the ground state of the system. A computational problem is mapped onto an array of cells by the layout of the cells, where the goal is to make the ground state configuration of electrons represent the solution to the posed problem. Then computation becomes a task of applying a set of inputs that put the system into an excited state, and then letting it relax into a new ground state. For each set of inputs a unique system ground state exists that represents the solution for those inputs. The mapping of a combinational logic problem onto a QCA system can be accomplished by finding arrangements of QCA cells that implement the basic logic functions AND, OR, and NOT. An inverter, or NOT, is shown in Fig. 3(b). In this inverter, the input is first split into two lines of cells then brought back together at a cell that is displaced by

[a]Electronic mail: snider.7@nd.edu

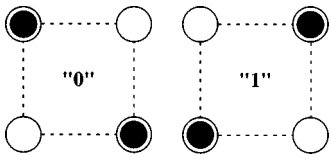

FIG. 1. Basic four-dot QCA cell showing the two possible ground-state polarizations.

45° from the two lines, as shown. The 45° placement of the cell produces a polarization that is opposite to that in the two lines, as required in an inverter. AND and OR gates are implemented using the topology shown in Fig. 3(c), called a majority gate. In this gate, the three inputs ''vote'' on the polarization of the central cell, and the majority wins. The polarization of the central cell is then propagated as the output. One of the inputs can be used as a programming input to select the AND or OR function. If the programming input is a logic 1 then the gate is an OR, but if a 0 then the gate is an AND. Thus, with majority gates and inverters it is possible to implement all combinational logic functions. Memory can also be implemented using QCA cells,[5] making general purpose computing possible.

Some additional explanation is necessary for the fan-out structure shown in Fig. 3(d), which was also employed in the inverter. When the input of one of these structures is flipped, the new ground state of the system is achieved when all of the cells in both branches flip. The problem is that the energy put into the system by flipping the input cell is not sufficient to flip cells in both branches, leading to a metastable state where not all of the cells have flipped. This is not the ground state of the system, but can be a very long-lived state, leading to erroneous solutions in a calculation. Avoiding these metastable states is simply a matter of switching the cells using a quasiadiabatic approach, which keeps the system in its instantaneous ground state during switching, thus avoiding any metastable states. Details of quasi-adiabatic switching have been published previously.[2,6] Quasi-adiabatic switching can be implemented in both semiconductor and metallic QCA systems.

As an example of more complex QCA arrays, consider the implementation of a single-bit full adder shown in Fig. 4, using majority gates and inverters. A full quantum mechanical simulation of such an adder has been performed,[4] verifying that it yields the correct ground state output for all eight possible combinations of the three inputs. As mentioned earlier, this adder, implemented using dots on 20 nm centers, would occupy an area of 1 μm^2, approximately the same area to be occupied by a single 0.07 μm gate-length transistor in 2010. A QCA array like the adder works because the layout of the quantum-dot cells has provided a mapping between the physical problem of finding the ground state of the cells and the computational problem.

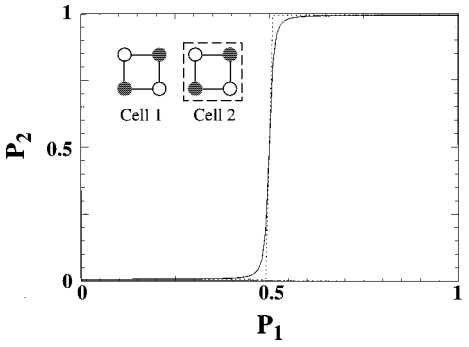

FIG. 2. Bistable cell polarization. As the polarization of cell 1 is changed linearly from 0 to 1, the polarization of cell 2 changes abruptly.

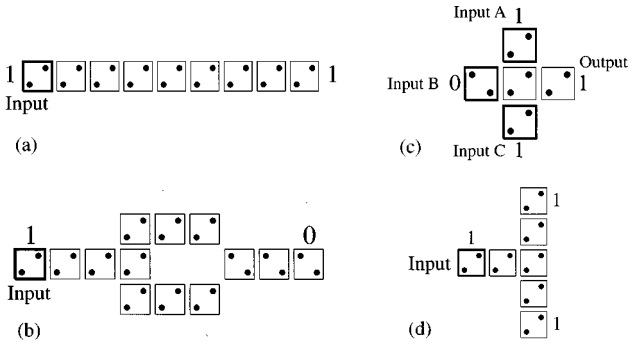

FIG. 3. (a) Line of QCA cells. (b) QCA inverter. (c) QCA majority gate. (d) Fanout.

II. EXPERIMENT

The experimental work presented is based on a QCA cell using aluminum islands and aluminum-oxide tunnel junctions, fabricated on an oxidized silicon wafer. The fabrication uses standard electron beam lithography and dual shadow evaporations to form the islands and tunnel junctions.[7] A completed device is shown in the scanning electron micrograph (SEM) of Fig. 5. The area of the tunnel junctions is an important quantity since this dominates island

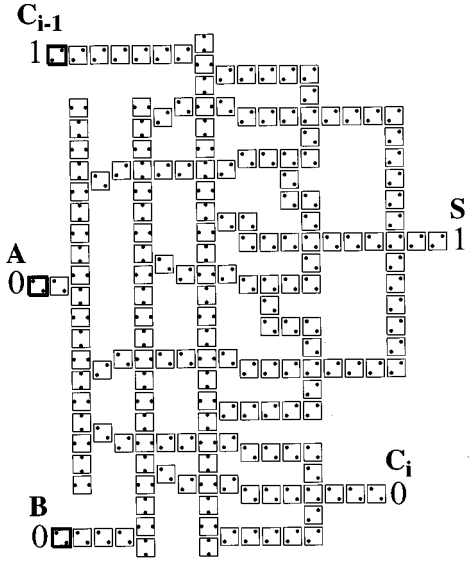

FIG. 4. QCA full adder.

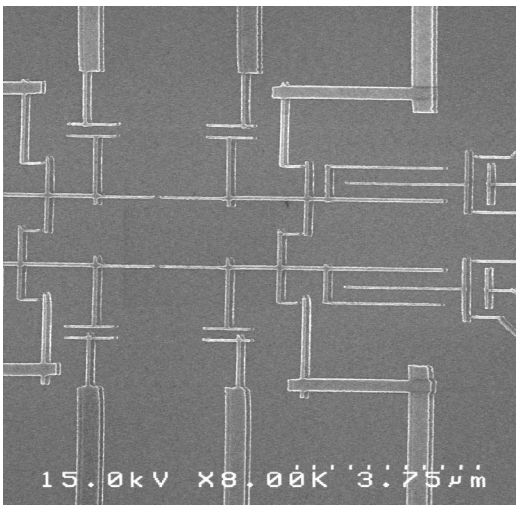

FIG. 5. SEM of QCA cell and electrometers.

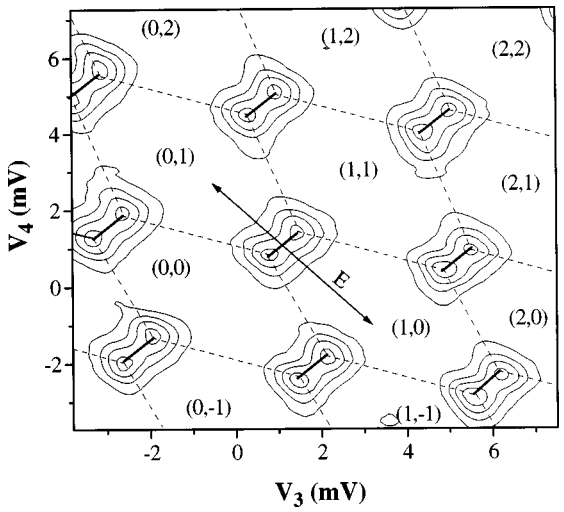

FIG. 7. Contour plot of the conductance through the output half-cell D3–D4. The arrow marked E denotes the transition where an electron moves from one dot to the other within the half-cell.

capacitance, determining the charging energy of the island, and hence the operating temperature of the device. For our devices, the area is approximately 60×60 nm, giving a junction capacitance of 400 aF. These metal islands stretch the definition of a quantum dot, but we will refer to them as such because the electron population of the island is quantized and can be changed only by quantum mechanical tunneling of electrons.

We recently demonstrated the first step in the development of QCA systems, a functional QCA cell where we can switch the polarization of a cell. This confirms the basic premise of the QCA paradigm: that the switching of a single electron between coupled quantum dots can control the position of a single electron in another set of dots.[8,9] A simplified schematic diagram of our latest QCA system is shown in Fig. 6. The four-dot QCA cell is formed by dots D1–D4, which are coupled in a ring by tunnel junctions. A tunnel junction source or drain is connected to each dot in the cell. This implementation is an improvement over earlier designs in that the tunnel junctions coupling D1–D3 and D2–D4 provide a capacitance more than twice as large as the lithographically defined capacitance used previously.[9] A larger capacitance is expected to improve the bistability of the cell.

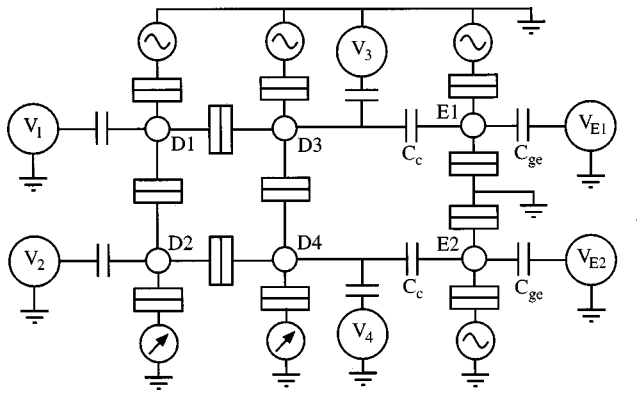

FIG. 6. Simplified schematic of the four-dot QCA cell with electrometers.

The two individual dots E1 and E2 are used as electrometers. The device is mounted on the cold finger of a dilution refrigerator that has a base temperature of 10 mK, and characterized by measuring the conductance through various branches of the circuit using standard alternating current lock-in techniques. A magnetic field of 1 T was applied to suppress the superconductivity of the aluminum metal. Full details of the experimental measurements are described elsewhere.[8–11]

The operation of a QCA cell is best understood by examining the conductance through each double-dot half-cell, D1–D2 and D3–D4. Consider first the conductance through the output half-cell as a function of the two gate voltages V_3 and V_4, as shown in the contour plot of Fig. 7. A peak in the conductance is observed each time that the Coulomb blockade is lifted for the double-dot system. Due to the capacitive coupling between the dots, each peak splits into a double peak. These peaks form the vertices of a hexagonal structure that we refer to as the ''honeycomb,'' delineated by the dotted lines in Fig. 7.[12] The electron population of the dots is stable within each hexagon of the honeycomb and changes when a border between cells is crossed. The excess electron population within each hexagon can thus be labeled, with the (0,0) hexagon centered at $V_3=V_4=0$ V. A point in the honeycomb defined by a single setting of V_3 and V_4 is called the working point, which defines a particular configuration of electrons. If V_3 is swept in the positive direction with V_4 fixed, electrons are added one by one to the top dot as the working point moves horizontally through the hexagons (1,0) then (2,0) and so on. If V_4 is swept positive, electrons are added to the bottom dot as the working point moves vertically through the hexagons (0,1) and (0,2). Most important for QCA operation is motion of the working point in the direction shown by arrow E in Fig. 7. This movement between the (0,1) and (1,0) hexagon represents the switching of an electron between the bottom dot and top dot. The goal of our experiment is to demonstrate QCA operation by using electrodes to force this transition in the input half-cell, D1–

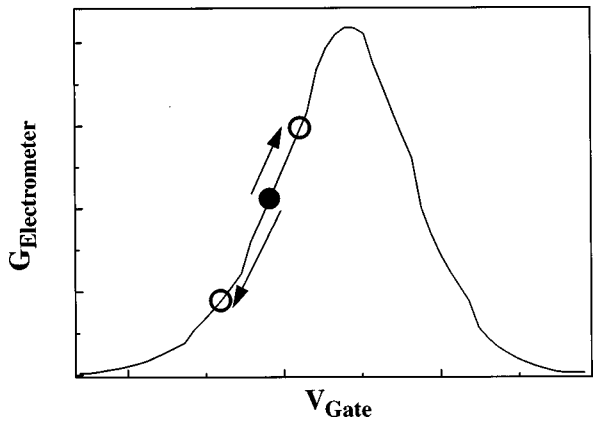

FIG. 8. Electrometer operation. Small potential variations coupled to the electrometer can cause large changes in the conductance.

D2, which in turn forces an opposite transition in the output half-cell, D3–D4.

Since the operation of a QCA cell depends on the position of a single electron, it is necessary to track the position of electrons within the cell. One way to accomplish this is to measure the conductance through each half-cell. A peak in the conductance as the gate voltages are changed indicates that the Coulomb blockade has been lifted for both dots simultaneously, and a change in the dot population has occurred. However, as seen in Fig. 7, not all electron transitions can be detected in this manner. For instance, if V_3 alone is swept, electrons are added to only the top dot, and no change in the conductance through the dots is seen. To fully characterize the QCA cell it is therefore necessary to externally detect the charge state of each dot individually. This is done using the electrometer dots E1 and E2,[11] capacitively coupled to the output half-cell, as shown in the schematic of Fig. 6. Each electrometer operates by detecting small potential changes in the dot being measured. The operating principle of a single-dot electrometer is illustrated in Fig. 8, which shows a single conductance peak of the electrometer. In the simplest electrometer measurement, the gate voltage is adjusted so that the working point lies on the side of this conductance peak, then held constant. Current through the electrometer is measured using a low noise, low offset, current preamplifier and lock-in amplifier with a small (10–20 μV) excitation at a frequency of 10–200 Hz. Any potential variations coupled to the electrometer, such as those on a nearby dot, will act as an additional gate voltage to the electrometer dot that causes a shift of the working point, shown in Fig. 8. Since the conductance peaks are quite sharp, a small change in the gate voltage gives a large change in the conductance through the electrometer dot. Knowing the capacitance that couples the electrometer to the dot, and the shape of the electrometer conductance peak, it is possible to calculate the potential on the measured dot. This measurement technique, though simple, has several disadvantages. In order to induce a strong signal in the detector the coupling capacitance has to be relatively large. In this case, however, the charge state of the measured cell can be affected by the changing potential of the electrometer. Also, the sensitivity and linearity of this detection method are strong functions of temperature and bias point.

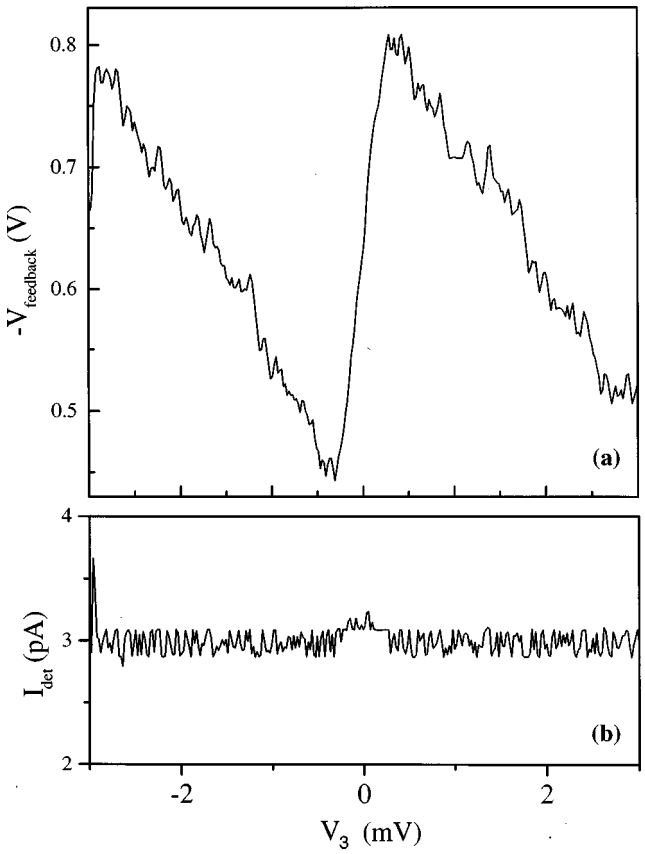

FIG. 9. (a) Electrometer feedback voltage, proportional to the dot potential. (b) Electrometer current, kept nearly constant by the feedback.

To improve the detection scheme we implement a noninvasive detector, using a software-based proportional-integral feedback loop that keeps a constant current through the electrometer, similar to a hardware implementation used by Lafarge.[13] With the feedback loop open the bias on the electrometer gate is adjusted to bring the electrometer to a point of maximum sensitivity, as before, but when the loop is closed the electrometer current is kept constant by adjusting the electrometer gate bias. The dot potential can be calculated from the feedback voltage using the simple expression $V_{\mathrm{dot}} = -V_{\mathrm{fb}} C_{\mathrm{ge}} / C_{\mathrm{c}}$, where C_{ge} is the electrometer gate capacitance, and C_{c} the coupling capacitance between dot and electrometer. For a differential QCA measurement, it is vitally important that E1 and E2 be identical electrometers.[14] The noninvasive electrometers are ideal for this purpose because the feedback removes the dependence on the shape of the electrometer current peak. Instead, the electrometer characteristics depend only on lithographically defined capacitors which have a well-controlled and stable value . Because of the high ''open loop gain,'' the electrometer is linear, keeps the same sensitivity over the wide range of temperatures, and most importantly, keeps the electrostatic potential of the electrometer constant, thus preventing it from affecting the cell. Time constants of the feedback were optimized to ob-

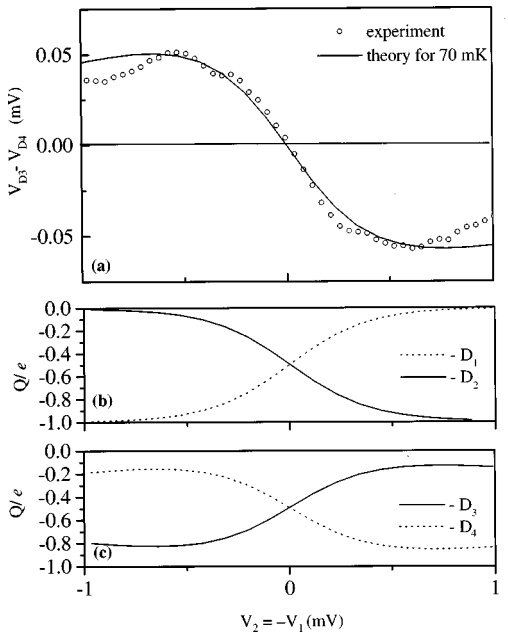

FIG. 10. (a) Differential potential in the output half-cell, $V_{D3}-V_{D4}$. (b) Dot charge on the input half-cell, D1 and D2. (c) Dot charge on the output half-cell, D3 and D4.

tain the best settling time, without overshoot, for a typical scan rate. Figure 9(a) shows the results of a potential measurement of a dot within the cell, and Fig. 9(b) shows the current through the electrometer. The feedback loop keeps the current constant at the selected value of 3 pA, and the gate voltage can be used to calculate the dot potential and detect the motion of an electron within the cell.

QCA operation is demonstrated by biasing the cell, using the gate voltages, so that an excess electron is on the point of switching between dots D1 and D2, and a second electron is on the point of switching between D3 and D4. A differential voltage is then applied to the input gates V_1 and V_2 ($V_2=-V_1$), while all other gate voltages are kept constant. As the differential input voltage is swept from negative to positive, the electron starts on D1, then moves from D1 to D2. This forces the other electron to move from D4 to D3. The experimental measurements confirm this behavior. Using the electrometer signals we can calculate the differential potential in the output half-cell, $V_{D3}-V_{D4}$, as a function of the input differential voltage. This is plotted in Fig. 10(a), along with the theoretically calculated potential at a temperature of 70 mK. Although at a temperature of 0 K the potential changes are abrupt, the observed potential shows the effects of thermal smearing, and the theory at 70 mK shows good agreement with experiment. The heating of the electron system to temperatures above the 10 mK of the dilution refrigerator is likely due to the applied excitation voltage and noise voltages coupled into the sample by the leads. This effect is commonly seen in measurements of this type.[15] Figures 10(b) and 10(c) plot the theoretical excess charge on each of the dots in the input and output half-cells at 70 mK. This shows an 80% polarization switch of the QCA cell and confirms the polarization change required for QCA operation. The polarization is less than 100% due to thermal smearing. It is this smearing that limits the operating temperature of the QCA system. The polarization decreases when the thermal energy, kT, is sufficient to drive the cell into the wrong polarization some portion of the time. For QCA cells such as the one presented here, a maximum of five cells could be connected before an error state becomes statistically favorable. Larger QCA systems will require a greater energy separation between the ground state and excited states. This can be achieved by reducing the capacitances in the system

III. SUMMARY

A device paradigm based on QCA cells offers the opportunity to break away from FET based logic and to exploit the quantum effects that come with small size. In this new paradigm, the basic logic element is no longer a current switch, but a small array of quantum dots, and the logic state is encoded as the position of electrons within a quantum dot cell. We have demonstrated the operation of a QCA cell fabricated in aluminum islands with aluminum oxide tunnel junctions where the polarization of the cell can be switched by applied bias voltages. QCA cells are scalable to molecular dimensions, and since the performance improves as the size shrinks, a molecular QCA cell should operate at room temperature.

ACKNOWLEDGMENTS

This work was supported by the Defense Advanced Research Projects Agency, Office of Naval Research, and the National Science Foundation.

[1]C. S. Lent, P. D. Tougaw, W. Porod, and G. H. Bernstein, Nanotechnology **4**, 49 (1993).
[2]C. S. Lent and P. D. Tougaw, Proc. IEEE **85**, 541 (1997).
[3]C. S. Lent and P. D. Tougaw, J. Appl. Phys. **74**, 6227 (1993).
[4]P. D. Tougaw and C. S. Lent, J. Appl. Phys. **75**, 1818 (1994).
[5]T. J. Fountain and C. S. Lent (unpublished).
[6]P. D. Tougaw and C. S. Lent, J. Appl. Phys. **80**, 4722 (1996).
[7]T. A. Fulton and G. H. Dolan, Phys. Rev. Lett. **59**, 109 (1987).
[8]A. O. Orlov, I. Amlani, G. H. Bernstein, C. S. Lent, and G. L. Snider, Science **277**, 928 (1997).
[9]I. Amlani, A. O. Orlov, G. L. Snider, C. S. Lent, and G. H. Bernstein, Appl. Phys. Lett. **72**, 2179 (1998).
[10]G. L. Snider, A. O. Orlov, I. Amlani, G. H. Bernstein, C. S. Lent, J. L. Merz, and W. Porod, Semicond. Sci. Technol. **13**, 130 (1998).
[11]I. Amlani, A. O. Orlov, G. L. Snider, C. S. Lent, and G. H. Bernstein, Appl. Phys. Lett. **71**, 1730 (1997).
[12]H. Pothier, P. Lafarge, P. F. Orfila, C. Urbina, D. Esteve, and M. H. Devoret, Physica B **169**, 573 (1991).
[13]P. Lafarge, Ph.D. thesis, University of Paris, 1993.
[14]I. Amlani, A. O. Orlov, G. L. Snider, and G. H. Bernstein, J. Vac. Sci. Technol. B **15**, 2832 (1997).
[15]P. Lafarge, H. Pothier, E. R. Williams, D. Esteve, C. Urbina, and M. H. Devoret, Z. Phys. B **85**, 327 (1991).